Design and Development of an Aircraft Electric Powertrain Test Stand

Ayush Jha*, Virinchi Puligundla†, Jonathan Paravano‡ and Brian German§
Georgia Institute of Technology, Atlanta, GA, 30332

Recent advancements in battery technology and power electronics are enabling novel approaches to powered flight that rely on fully electric or hybrid-electric powertrain systems. To mitigate the risk surrounding such unproven systems, it is necessary to characterize their performance on a component-wide and system-wide basis. In this paper, we discuss the design and development of an electric powertrain test stand that can collect high-fidelity data of motor, controller, and battery performance, thereby allowing us to determine system performance, efficiencies, and thermal characteristics.

I. Nomenclature

ADC	=	Analog-to-Digital Converters
CAN	=	Controller Area Network
$cDAQ$	=	CompactDAQ
DC	=	direct current
EMI	=	electromagnetic interference
HV	=	high voltage
LV	=	low voltage
NI	=	National Instruments
$PMSM$	=	permanent magnet synchronous motor
PWM	=	pulse width modulation
RPM	=	revolutions per minute
$SPST-NO$	=	single pole - single throw normally open
VI	=	Virtual Instrument

II. Introduction

As electric powertrain technologies have matured in the automotive industry, their application in powered flight has gained attention across the aerospace industry. Electric powered aircraft promise numerous benefits over the current generation of fossil-fuel powered aircraft, including improvements in efficiency, increased flexibility in propulsor placement, and a reduction in emissions [1]. Before electric powertrain technologies can be implemented, however, it is crucial to test their capabilities to better understand how the components of the system perform and interact with one another. To make this possible, an electric powertrain test stand has been designed and built in the Daniel Guggenheim School of Aerospace Engineering at Georgia Tech. The stand is designed with the intent to test a wide variety of technologies relevant to electric aircraft powertrains including batteries, motors, motor controllers, and propellers. The need for modularity has driven design decisions which will allow users to swap out test articles to test a variety of motor, controller, battery, and propeller combinations.

The stand is designed with the capability to test motors in the 50kW category and with propellers up to 6 ft. in diameter. The system is powered by a programmable, bi-directional DC power supply that is capable of mimicking battery discharge curves and can deliver up to 54kW to the system. The modular design of the stand means that the power supply can be swapped out for a larger power supply or batteries if required for specific tests. Additionally, the

*Research Engineer I, Daniel Guggenheim School of Aerospace Engineering, AIAA Member
†Graduate Research Assistant, Daniel Guggenheim School of Aerospace Engineering
‡Graduate Research Assistant, Daniel Guggenheim School of Aerospace Engineering
§Associate Professor of Aerospace Engineering and Co-Director of Center for Urban and Regional Air Mobility, AIAA Associate Fellow

power supply can act as a load, therefore allowing users to study battery discharge performance without interacting with other elements of the system. Highly accurate current and voltage sensors are accompanied by a multi-axis force and torque transducer to monitor the thrust, torque, currents, and voltages delivered by and to the system. This allows users to accurately calculate system efficiencies and better understand the interactions between subsystems that form the overall powertrain.

III. System Development Process

A. Stand Design

The design for the physical test stand began with formalizing the requirements. The need to spin a six foot diameter propeller, measure thrusts up to 350 lb_f and measure torques up to 1650 lb_f-in were the primary design drivers. Fig. 1 shows the overall design of the stand and its dimensions.

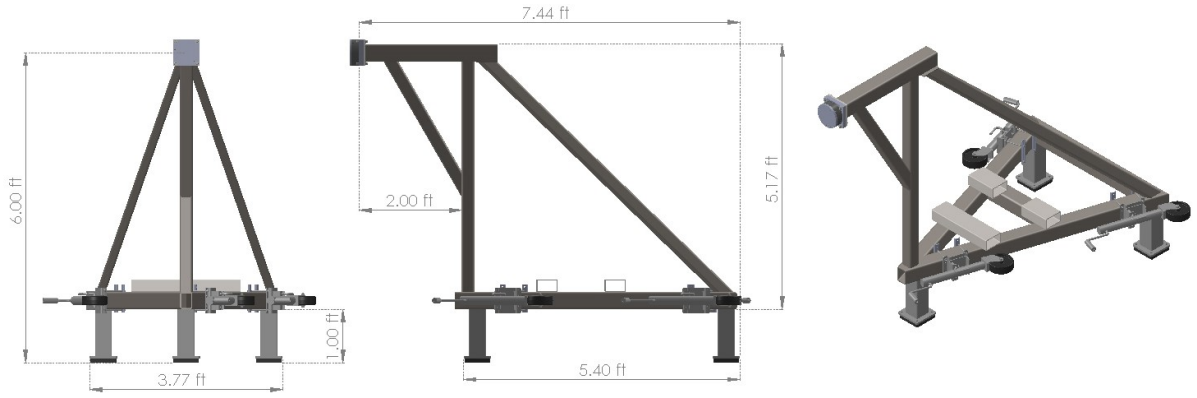

Fig. 1 Test stand design with dimensions

As illustrated in the figure, the designed structure provides a stiff load path while minimizing obstruction to the rotor wake. Welded mild steel rectangular tubing forms the structure, providing strength and ease of manufacturing at a low cost. The stand is designed with a triangular chassis to transfer forces from the superstructure to the legs. This superstructure consists of five tubes: a vertical member, horizontal member, a front brace, and two rear struts. The vertical and horizontal members cantilever the load cell attachment point in front of the test stand, reducing the aerodynamic influence of the chassis and struts. The front brace limits twisting in the horizontal member and the rear struts reduce bending in the vertical member. The superstructure members are laid out in the configuration shown in Fig. 1 to minimize the frontal area in the rotor wake and hence any associated interference. To allow safe testing, the legs mount the chassis to the test pad using bolts which run through vibration isolating rubber pads. Finite element analysis was conducted to size the structural members for the expected loads, and modal analysis showed negligible issues with excitation. The motor under test mounts to the load cell using a machined attachment and the controller is mounted onto the front brace to minimize the length of cabling between the test articles. Forklift slots and wheeled leveling jacks attached to the stand allow it to be moved to storage when not in use.

B. Initial Test Articles

To test the functioning of the test stand and validate its capabilities, an existing, commercially available powertrain system was needed. Following a review of available options, the motor and accompanying controller were sourced from Pipistrel (Pipistrel, Ajdovscina, Slovenia). The chosen motor is an air-cooled, axial flux permanent magnet synchronous motor (PMSM) designed specifically for use in electric aircraft, capable of delivering up to 40kW of shaft power. The accompanying controller is a liquid-cooled, variable frequency drive that is compatible with different position sensors and communicates with the operator via a controller network area (CAN) bus. While the remainder of the system development process described in the following sections was performed using these test articles, the modularity of the stand design means that both components can be swapped out for other test articles.

C. Power Supply Selection

To enable testing of powertrain systems without batteries, a programmable power supply was needed. This would allow users to conduct long duration testing runs at a range of voltage, current and power levels. The chosen power supply is a 54kW capable, programmable, bi-directional DC source and sink manufactured by Regatron (Regatron AG, Rorschach, Switzerland). As a source, the supply offers the ability to simulate battery discharge curves through a programmable output. As a sink, the supply enables testing of regenerative systems and can also behave as a programmable load for battery testing. Lastly, the power supply has a modular design which allows expandability to higher power levels if needed. While the power supply offers users the ability to test powertrain systems without batteries, they can be swapped in to conduct full powertrain system tests.

D. Sensor and Load Cell Selection

To collect the data needed to characterize the performance of the test articles, it is crucial to have accurate, reliable, and low-noise sensors installed on the test stand. For load measurements, both thrust and torque values are necessary to fully capture the performance of a propeller and motor combination. For the current and voltage sensors, low-noise, high accuracy measurements are needed to carry out efficiency calculations of components in the system.

A study of commercially available force and torque transducers was conducted to identify the appropriate option for our needs. The need for both torque and thrust measurements meant that a transducer capable of measuring multi-axis loads and torques was needed. The Omega160 F/T sensor manufactured by ATI (ATI Industrial Automation, NC, USA) was chosen due to its ability to measure forces in all three Cartesian axes and torques about each axis with a high signal to noise ratio. Multiple calibration settings were acquired to allow flexibility in the sensing ranges and the measurement resolution.

To determine system efficiencies, the electrical power into the system is compared against the mechanical power output by the motor. High accuracy current and voltage sensors are used to determine the DC power into the controller from the power source. On the output side, the electrical power delivered by the controller is difficult to measure due to the pulse width modulation (PWM) of phase currents done by the controller [2]. As a result, we do not measure the AC phase currents and voltages output by the controller and its standalone efficiency is not captured. The mechanical output power from the motor is derived from the torque measurements reported by the load cell and the RPM measurements reported by the controller. Hence the overall motor and controller system efficiency is calculated using Eq. (1) where τ is the motor torque in Nm, $\dot{\theta}$ is the motor rotational speed in rad/s, V_{DC} is the DC voltage into the controller and I_{DC} is the DC current into the controller.

$$\text{System Efficiency} = \frac{P_{out,shaft}}{P_{in,controller}} = \frac{\tau \times \dot{\theta}}{V_{DC} \times I_{DC}} \tag{1}$$

Numerous voltage and current sensors were reviewed with a focus on performance in high EMI environments. The CV3-1500 voltage transducer and the LA 205-s current transducer manufactured by LEM (LEM International SA, Meyrin, Switzerland) were selected due to their accuracy, immunity to external interference and galvanic isolation between the primary and secondary circuits. The RPM measurements are provided directly by the controller but can also be measured externally by an optical tachometer. Additionally, the controller also provides temperature readings, one for the windings in the motor and another for it's own internal circuitry, allowing test article temperatures to be monitored during runs.

E. Electrical Systems Design

Given the inherent hazards present when dealing with kilowatt level power systems, it is crucial to design a safe, reliable and fault-tolerant high voltage connection between the power source and the motor and controller. At the same time, reliable and isolated low voltage busses are needed to power the sensors and the safety systems used to monitor and control the operations of the test stand.

1. High Voltage System Design

The design of the high voltage system focuses on safety, with multiple disconnects installed to allow operators to safely halt testing when needed. A review of existing powertrain systems was conducted alongside consultations with experts from academia and industry before undertaking the design. Fig. 2 shows a schematic of the high voltage bus for the test stand.

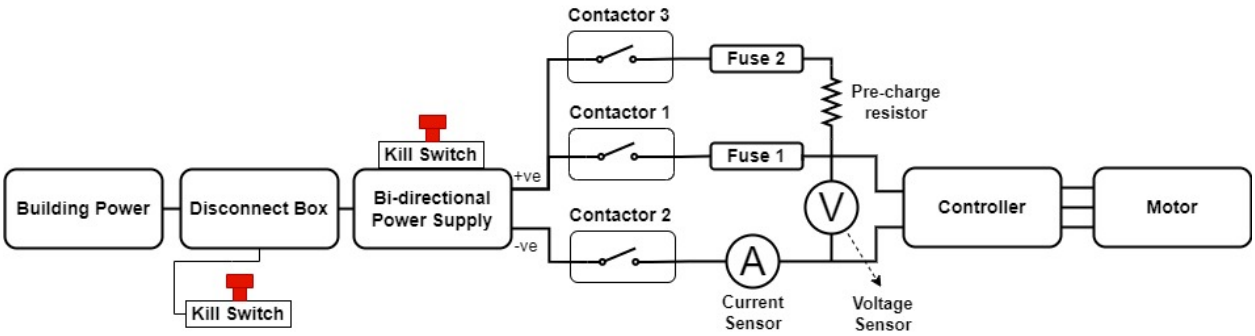

Fig. 2 High voltage system schematic

As shown, the high voltage bus employs a combination of kill switches, fuses and contactors to regulate the connection between the power source and controller. Fast-blow fuses installed between the power supply and the load protect the controller and motor in overcurrent situations. These fuses can be easily swapped out based on the voltage and current needs of the test being conducted. The high voltage contactors are switches that are used to isolate the HV power source from the rest of the system when needed. These devices are controlled by providing a low voltage control signal from the operator's desk and must be capable of performing at the current and voltage levels expected during tests. The contactors chosen for the stand are single pole - single throw normally open (SPST-NO) contactors that are rated to perform at up to 500A at 900VDC. This is well beyond the output capabilities of the power supply and ensures that the system can safely, reliably and repeatedly be isolated from the source when needed. Like the fuses, these contactors can be swapped out for higher rated ones if required.

The high voltage bus also features a pre-charge circuit which is essential when operating a capacitive load such as the motor controller. During power up, high voltage systems with downstream capacitance can cause large inrush currents which damage components, set-off circuit protection devices and weld shut contactor junctions in the closed position [3]. To prevent these issues, a pre-charge circuit is used to slowly charge the downstream capacitance of the controller. A resistor in line with the circuit regulates the current and can be swapped out based on the needs of the test being conducted. During initial power up of the test stand, contactors 2 and 3 are closed by the operator to allow the controller capacitor to charge. Once the capacitor is charged to 95 percent, contactor 1 can be closed, thereby safely connecting the load to the power supply. Since the resistance in the pre-charge circuit is higher, current will only pass through the main bus during test operations.

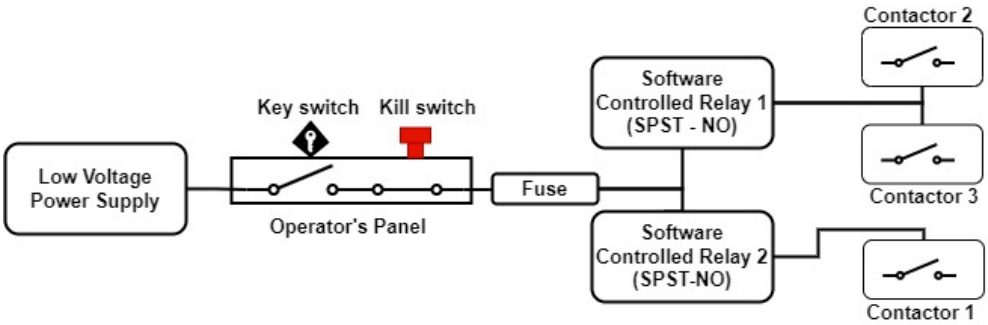

Fig. 3 Low voltage system schematic

2. Low Voltage System Design

The low voltage system for the test stand is responsible for powering the various sensors, transmitting their readings, and providing the control signals needed for opening and closing the contactors. The schematic in Fig. 3 shows the portion of the low voltage system that allows the test operators to control the contactors. As with the high voltage bus, the low voltage bus employs a combination of disconnects, fuses and relays to regulate the control of the contactors.

Since the contactors in the HV bus are in the normally open configuration, they require a low voltage command signal to close their junctions and complete the circuit. This voltage signal is provided by a low voltage power supply on the operator's desk. In line with this power supply is the operator's panel which houses a kill switch in the normally closed position and a key switch in the normally open configuration. Both these switches must be closed by the operator to complete the connection. Following these switches are two software controlled SPST-NO relays which are independently controlled by the test operator using the control software. The first of these relays connects to contactors 2 and 3, and the other to contactor 1. Closing the first relay completes the pre-charge circuit and allows the controller's capacitors to be charged. Once this is complete, the second relay can be closed to complete the HV bus. At any point during testing, the operator can trigger the kill switch, key switch or either software controlled relay to open the contactors and disconnect the load from the power source, thereby providing multiple ways to safely stop the system. Not pictured in the schematic are the low voltage busses providing DC power to the sensors and transmitting analog readings to the ADCs.

F. Data Acquisition and Control Interface

The data acquisition and control software for the test stand was developed using National Instruments (NI) (Austin, Texas) LabView and is divided into three main components: data analysis, measurement display, and control system. Each component consists of multiple Virtual Instruments (VIs) and subVIs to increase the modularity and readability of the software. The modular design of the software also makes it easier to debug any errors or issues that are discovered during the testing or integration process. The software design is based on [2] and similarly uses queues to combine data from multiple sources into a single pipeline for processing and transfer between multiple VIs. The overall software logic diagram is shown in Fig. 4.

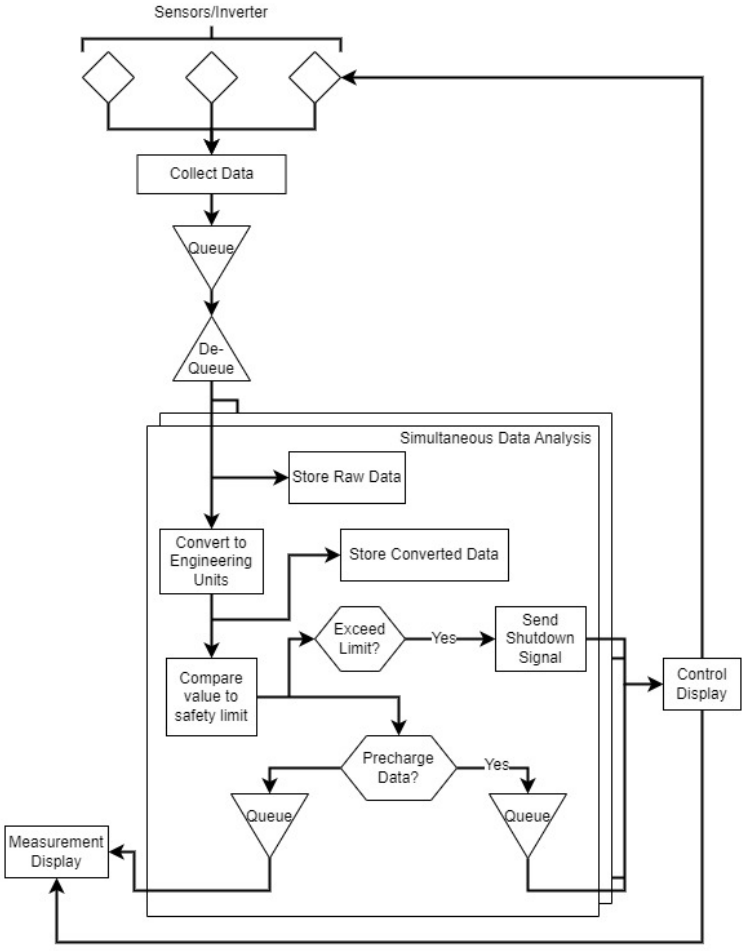

Fig. 4 Overall software logic diagram.

1. Data Acquisition

Data is acquired from the sensors and controller using two separate VIs because of the different modes of communication being used. The load cell, voltage and current sensors all connect directly to ADC cards in a NI CompactDAQ (cDAQ) chassis while the controller and power supply connect directly to the PC via CAN as shown in Fig. 5. The cDAQ chassis has eight slots in which various compatible modules can be inserted and connects to the PC via a single USB connection. The cDAQ chassis also helps controls the timing and synchronization across all connected modules which allows data to be collected at the same time at a user-selected sampling rate. In addition to the ADC cards, the cDAQ chassis also houses the SPST - NO software controlled relay module that is used to control the contactors. The data collected via the two VIs is combined into a single queue with a timestamp and sensor identifier to be processed by the data analysis VI. The sensor id is either the CAN id for a CAN message or a custom id based on the card and port a sensor is connected to on the cDAQ chassis.

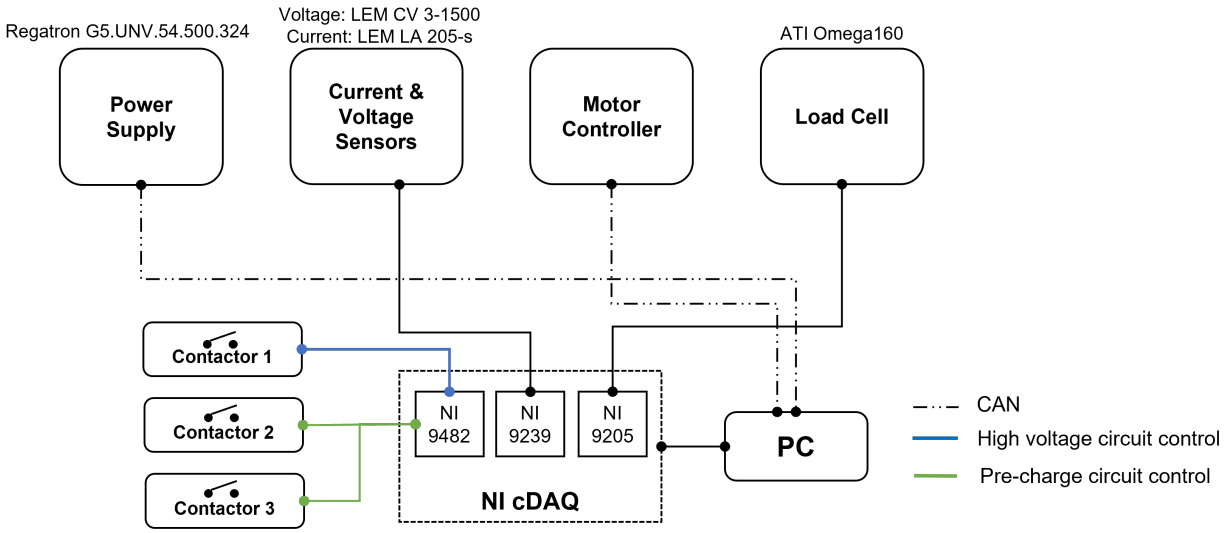

Fig. 5 Communication and control system diagram.

2. Data Analysis

The data analysis component has one main VI with multiple sub-VIs that handle individual parts of the analysis procedure. The main VI pops data packets from the queue and passes them to data conversion sub-VIs that convert the raw data to engineering units based on the sensor id of the data packet. To handle the large amounts of data being collected, multiple data conversion sub-VIs run simultaneously in parallel. From the data analysis VI, there is a control queue and a measurement queue that correspond to the control and measurement displays, respectively. All relevant converted data is added to the measurement queue while only the pre-charge data and shutdown signals are added to the control queue. Furthermore, any shutdown signal generated when a safety limit is exceeded is added to the front of the control queue to ensure that the shutdown procedure starts immediately after a safety limit has been exceeded.

To allow for small variations in data, the system has tiered safety limits with the lower tier resulting in shutting down the motor (Motor Zero) and the higher tier resulting in killing the entire system (KILL). The KILL tier is set to the maximum limit of the controller and motor under test and should not be exceeded at any time. The KILL limits are fixed for each controller/motor combination at the beginning of the test cycle and cannot be changed. The Motor Zero tier is the limit that should not be exceeded for a specific test. The limits in this tier are configurable and can be set from the control display for a certain test. For example, the RPM Motor Zero limit was set to a low value during the initial integration of the test stand since small torque values were being commanded to the motor. Based on which tier's safety limits have been violated, the corresponding shutdown signal is sent to the control display, and the appropriate automated shutdown procedure is triggered in the control system.

3. Control System

The Control Display shown in Fig. 6 is the frontend that the operator interacts with to control the entire test stand and is the main VI for the entire system. The Control Display VI is responsible for starting and shutting down all main VIs, creating all queues used between VIs, and establishing CAN bus communication. The Control Display has built-in safety features in the backend that prevent accidental commands that would perform an unsafe action. For example, LabView allows control buttons to be disabled, a feature that is used extensively in the software design to ensure that a control button cannot be accidentally activated. To illustrate this functionality, the startup procedure for the test stand will be discussed briefly. The first step is setting which control mode to use to control the motor: RPM or torque. Until this control mode is set, the "Motor Startup" button cannot be pressed and neither of the relays can be closed. Once the motor control mode is set, the "Motor Startup" button is enabled, and once the button is clicked, the "Precharge Relay" button is enabled. The "Precharge Relay" closes the relay that controls the precharge contactor, and the "Motor Relay" button is disabled until the precharge reaches 95%. After the "Motor Relay" button is closed, the respective control input that was chosen ("Motor Speed" or "Motor Torque") is enabled, and speed or torque commands can be given to the motor.

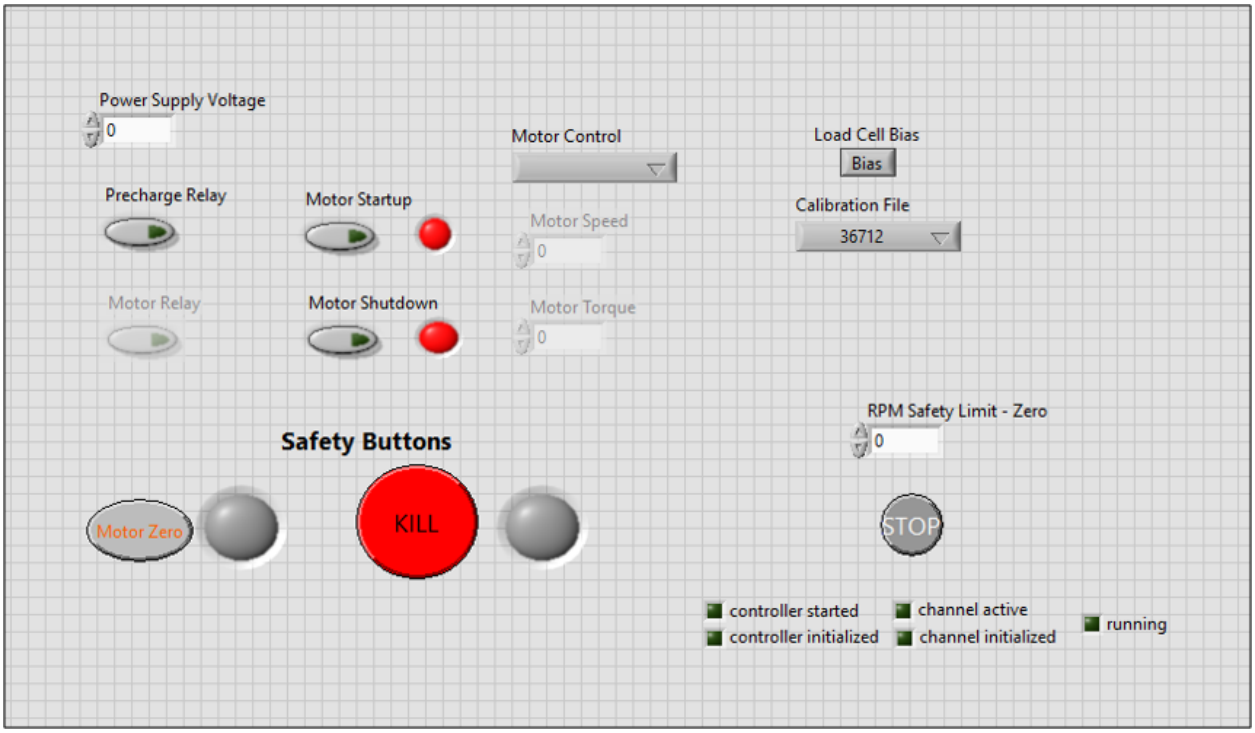

Fig. 6 System control interface for operator.

Another safety feature that is included in the Control Display is automated shutdown procedures. When a shutdown signal is received from the data analysis VI, the software automatically turns off the motor if the Motor Zero limits are violated or performs the KILL procedure if the KILL limits are violated. The KILL procedure for the system is to open all relays, turn off the motor, and set the power supply output voltage to 0V. The operator still has the capability to manually trigger the shutdown procedures by using the two safety buttons on the Control Display in case any irregular behavior is observed. In addition to the safety features, many other commands are automated in the backend such as the sequence of CAN messages required to start and stop communication with the motor.

4. Measurement Display

The Measurement Display, shown in Fig. 7, is the main display for information related to the test stand and was designed to allow an observer to know the state of the entire system from a single display. To accomplish this, the relay and KILL status is sent over from the Control Display, and all data that is collected from the sensors and controller is displayed with both the actual value and a rating from 0 to 10. The rating correlates to the tiered safety limits and helps

gauge how close a certain value is to a safety limit. The tiers on the Measurement Display and corresponding rating are Nominal (0 - 5), Warning (5 - 7.5), Motor Zero (7.5 - 10) and KILL (>10). The color of the rating dial also changes to make it easier to distinguish which region a value is within. In the Nominal range, the color is always green, and in the Warning range, the color changes from green at the lower end of the range to orange at the upper end of the range. In the Motor Zero range, the color changes from orange at the lower end of the range to red at the upper end of the range, and in the KILL range, the color is always set to red.

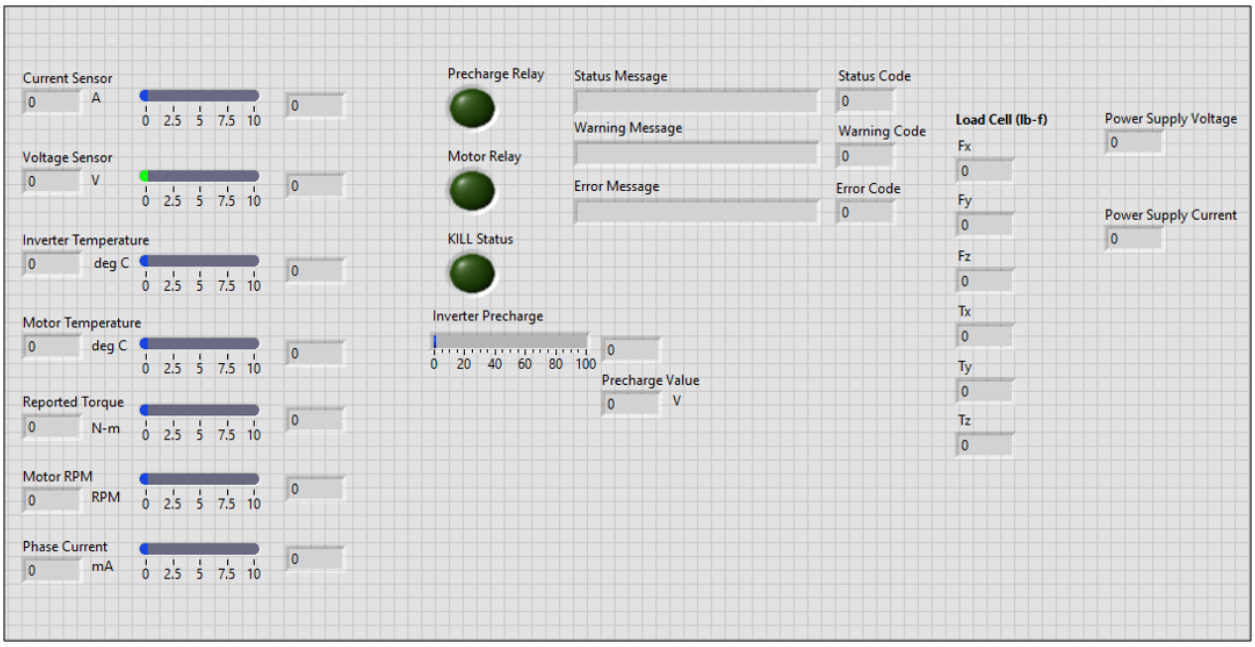

Fig. 7 Display of system information.

G. Liquid Cooling

The test stand also features liquid cooling abilities with a pump, reservoir, radiator and flow control valve. The valve allows the operator to adjust the flow rate, which is measured by a flowmeter, to the rate required to cool the components. Additionally, a temperature probe in the reservoir allows the operator to monitor the coolant's temperature while tests are being conducted. Fig. 8 illustrates the cooling loop, its components and the flow direction.

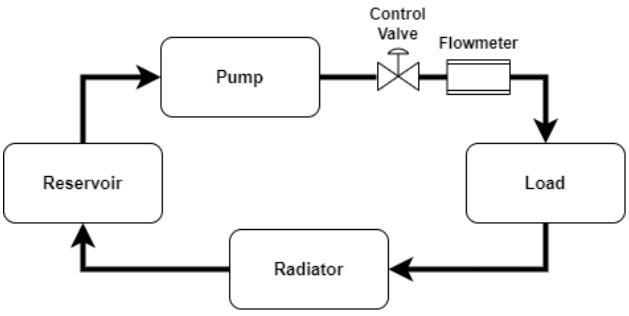

Fig. 8 Cooling loop schematic

IV. System Integration

The integration of the test stand and its various subsystems began with the construction of stand itself. AISI/SAE 4340 alloy steel tubes were welded together to form the superstructure which was powder coated to provide weather

resistance for outdoor testing. Fig. 9 shows the welded and powder coated test stand on the test pad prior to full integration.

Fig. 9 Physical stand on test pad

Next, individual subsystem components such as the load cell, sensors, contactors and relays were bench tested to ensure accuracy and validate the contactor control architecture. This approach enabled an incremental build-up and verified hardware performance prior to final installation. For the load cell, precision weights were used to apply known loads and to verify the device calibration matrices provided by the manufacturer. Similarly, the voltage and current sensors were tested by subjecting them to a range of known values. Fig. 10 and Fig. 11 show these respective bench tests being conducted. Following these tests, a representative circuit was built (Fig. 12) to test the contactors and their interaction with the low voltage system and the operator. Using the software provided by the relay manufacturer, both relays were cycled repeatedly to ensure the contactors could be controlled as designed. Similarly, the kill switch was also tested to ensure that it was a reliable circuit disconnect when necessary.

Following the individual component tests, the HV and LV busses were assembled and integrated to be mounted on the stand. To keep the system compact and easy to operate, all the HV bus components between the power supply and motor controller were mounted in a single enclosure (Fig. 13) and all LV cabling needed to power the sensors, transmit their readings, and control the contactors terminated at a common junction. To further reduce the complexity of the system and make the LV busses more manageable, the enclosure was mounted in a server rack with the accompanying components mounted on racks above it (Fig. 14). This approach allowed the power supplies for the sensors, the ADCs, and the software controlled relays to be housed close to the instruments they interact with. Furthermore, the power supply for the load cell and the CANbus hub were also mounted to the server rack, resulting in a single housing for all the instrumentation needed to operate and observe the test stand.

In parallel, software development and testing was carried out which followed a similar incremental approach as the hardware integration. During the software development, the communication interface with the NI cDAQ and controller were tested separately because of the different communication protocols used. The components connected to the cDAQ chassis (relays and contactors, voltage sensor, current sensor, load cell) were tested using the same approach described above in the hardware testing but with LabView acting as the control and measurement interface. The software used for this testing was developed in a separate VI to ensure that each segment of code worked as intended.

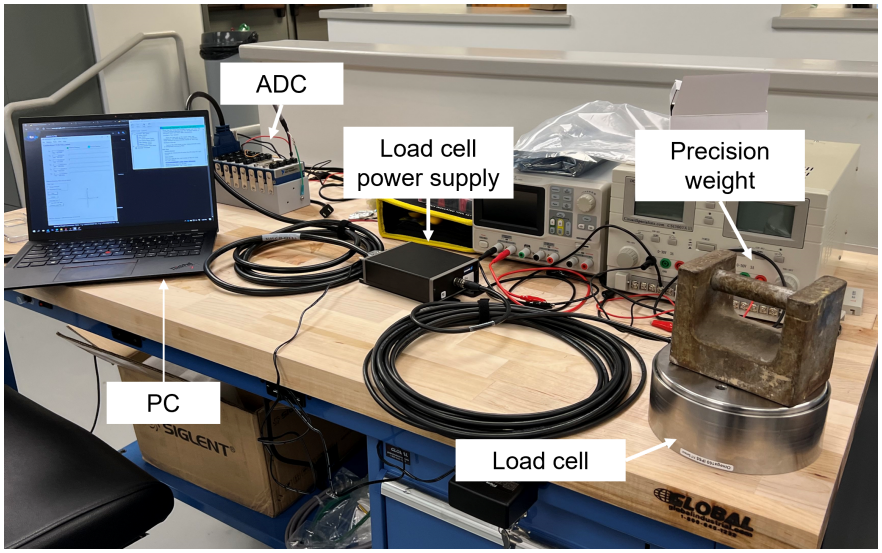

Fig. 10 Load cell bench testing

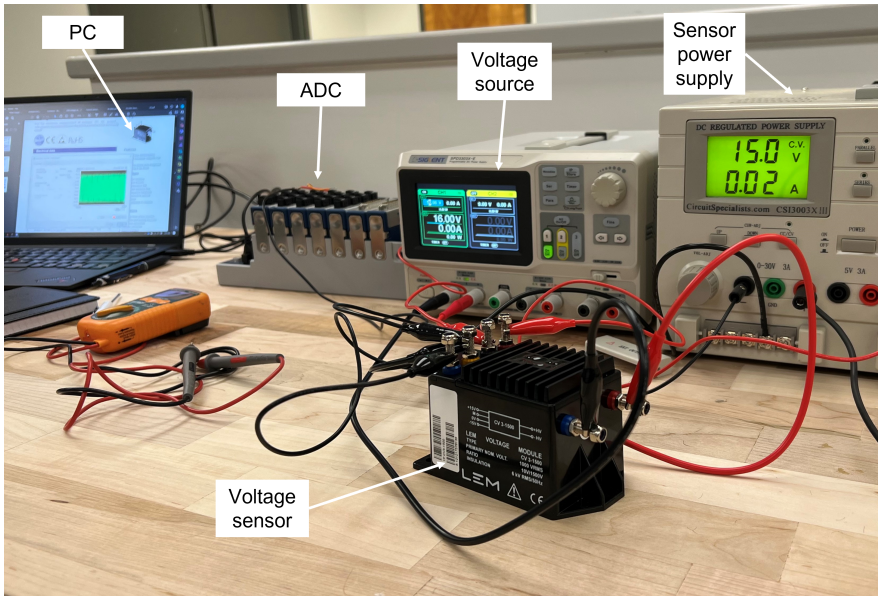

Fig. 11 Voltage sensor bench testing

For the CAN interface with the controller, the first step was to verify that communication could be established with the controller using LabView. For this purpose, the USB-to-CAN V2 adapter by Ixxat (HMS Networks, Halmstad, Sweden) was chosen because of its integration with LabView, and the CAN Bus analyzer tool by Microchip (Microchip Technology Inc., Chandler, Arizona) was acquired to passively log all messages sent on the bus. Ixxat provided a VI capable of sending single CAN messages with the adapter, so this VI was used for the first attempt at communicating with the controller. The CAN bus consisted of the controller, Microchip adapter, and a PC with LabView. Individual CAN frames from the controller's start-up procedure were manually sent using the VI provided by Ixxat. Once communication with the controller was established, the software was developed to take user input from the Control Display and generate the appropriate CAN frames. For this phase of the development, the CAN bus consisted of the Microchip adapter and a PC with LabView. The Microchip adapter logged every message sent from the Control Display, and each message was verified by manually converting the message from hex to decimal. In addition to logging messages, the Microchip adapter can send messages. This functionality was used to test the Measurement Display by sending messages with the

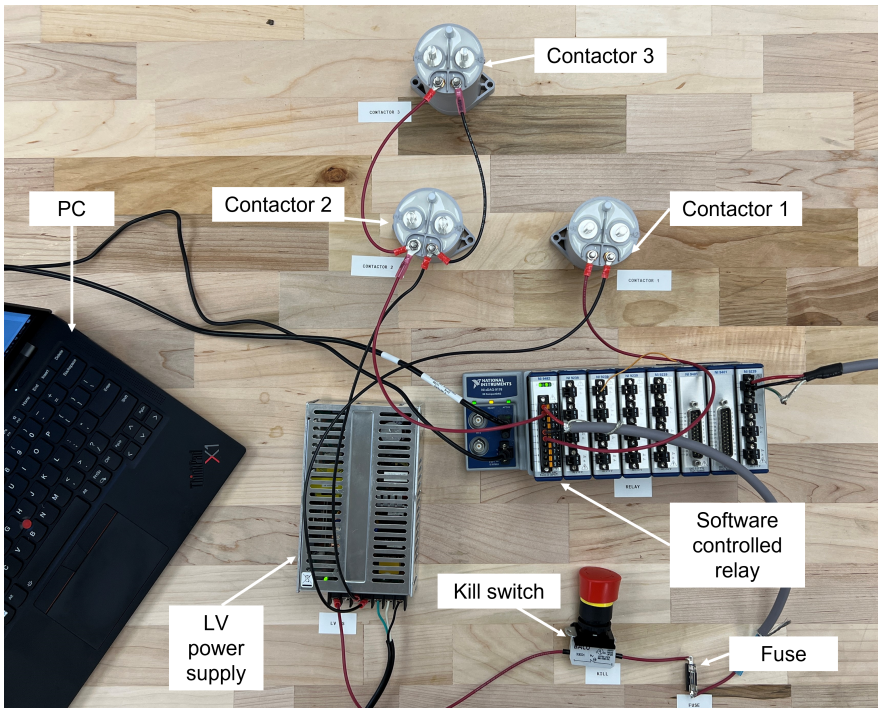

Fig. 12 LV control system bench testing

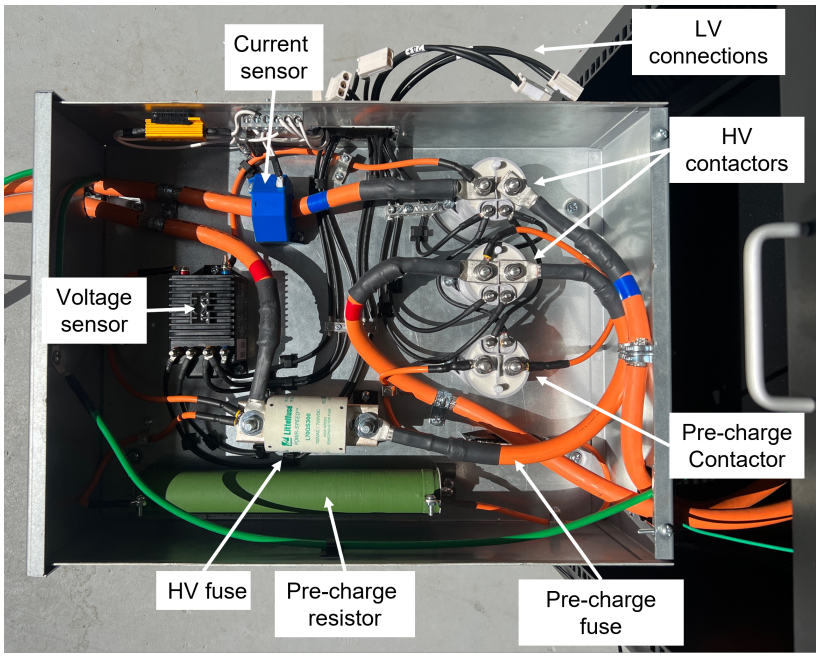

Fig. 13 HV systems enclosure mounted in server rack

Microchip adapter and verifying the correct conversion was being performed in LabView. The operator's table shown in Fig. 15 has the completed control and measurement displays on separate monitors for ease of use with an additional monitor for a live camera feed of the test stand.

Following the hardware integration and software testing, the initial test articles were integrated into the stand to begin systems testing (Fig. 16). An incremental testing approach was undertaken to ensure safe operations of all

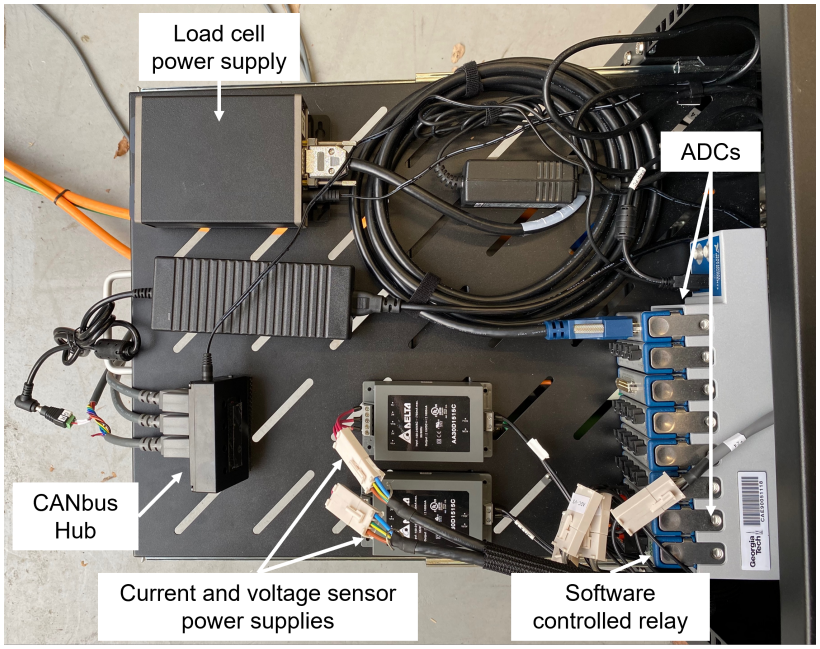

Fig. 14 LV and communication systems mounted in server rack

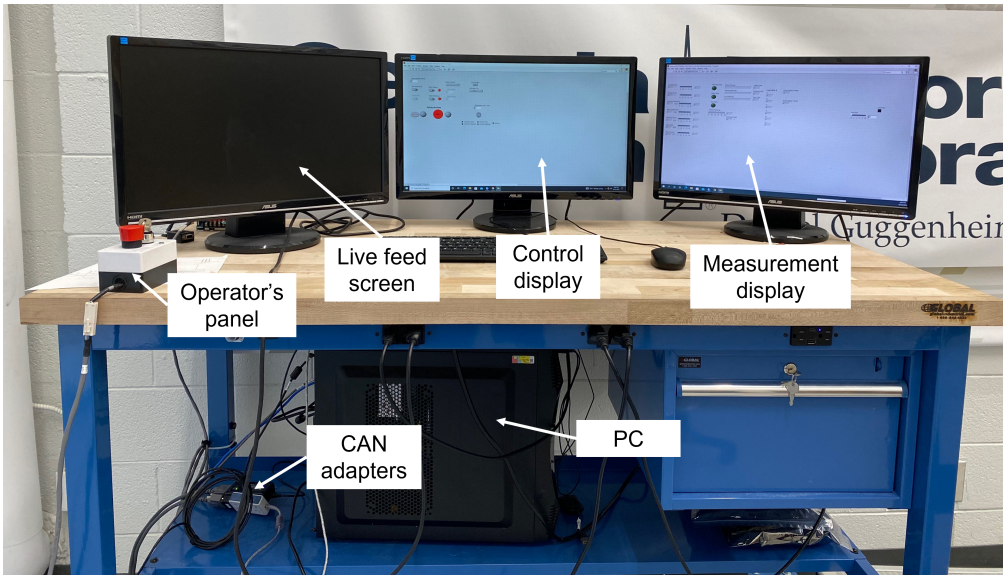

Fig. 15 Operator's table integrated with test stand.

systems. With zero motor torque commanded, the power supply was cycled through a range of voltages, and the behavior of the pre-charge circuit and voltage sensor was closely monitored. During the incremental testing approach, the Microchip adapter was connected to the CAN bus, and the software's CAN interface was tested using the logged messages. Similarly, each safety disconnect, including all mechanical and software kill switches, was tested to ensure reliable operation.

Upon successful integration and completion of static system tests, a full systems check was conducted by performing no-load testing. Through the operator's control VI, the motor was successfully commanded to spin at low torque and data from the various sensors was closely monitored. This test validated the data acquisition system, the control system, and the liquid cooling capabilities of the test stand.

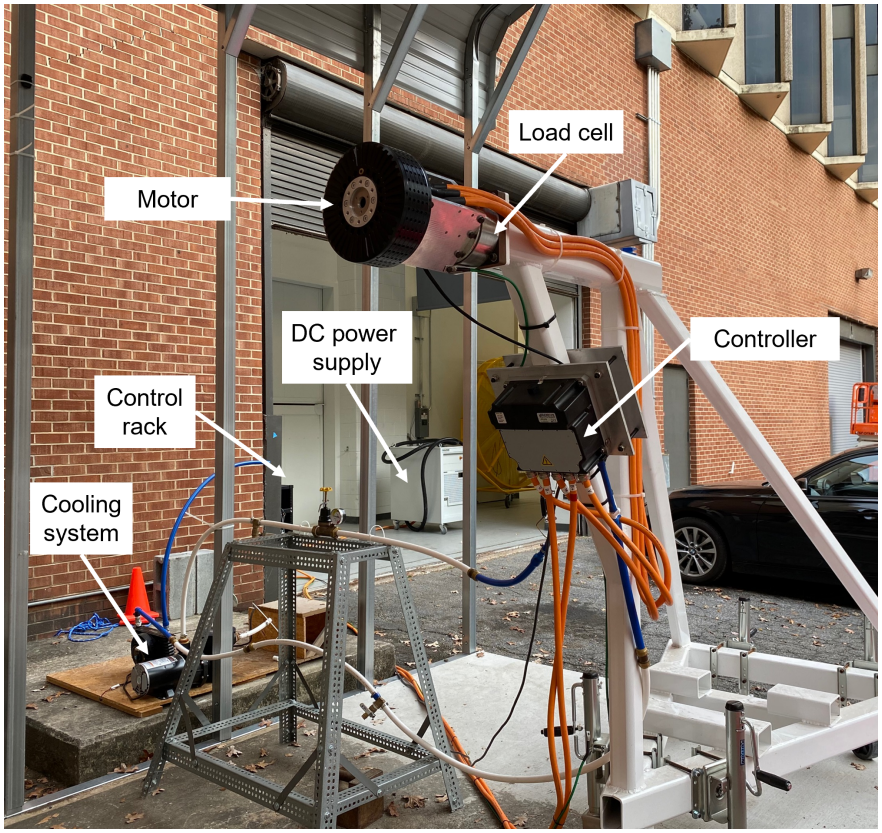

Fig. 16 Assembled test stand on test pad

V. Conclusions and Next Steps

To enable high fidelity testing of electric powertrain systems for aircraft, a test stand has been designed and built in the School of Aerospace Engineering at Georgia Tech. Designed with modularity in mind, the stand enables researchers to test combinations of motors, controllers, batteries and propellers to better understand their performance capabilities and the interactions between one another.

Work on the test stand is continuing, with an initial focus on continuing the calibration process and running tests under load with a propeller installed. To continue calibration of the load cell, as-installed thrust and torque testing is underway. Although previous bench testing discussed above was used for validation and calibration of the load cell, as-installed testing will help identify the effects of external interference on the installed load cell, if any.

After as-installed load cell calibration is complete, initial tests will be conducted using a two-bladed propeller to conduct measurements under load to validate system performance and to characterize any electromagnetic interference (EMI) that may affect test instrumentation.

Efforts are also underway to expand the capabilities of the test stand. These steps include the integration of a three-phase power analyzer to measure AC phase voltages and currents from the motor controller and a variable-pitch mechanism for the propeller.

As discussed above, the suite of sensors and load transducers currently implemented is sufficient for measuring the efficiency of the motor and motor controller as a system; however, the individual motor and controller efficiencies cannot be measured separately. To accurately capture these values, we are exploring the integration of a power analyzer to measure and record the three-phase power output by the controller. With these measurements, the power output from each of the components can be measured and hence their efficiencies can be determined.

The current system is only designed for fixed-pitch and ground adjustable fixed-pitch propellers. To further expand the test stand's capabilities, a variable pitch mechanism is being designed to allow testing of a wide range of in-flight variable pitch propellers and proprotors. This system will not only broaden the range of propellers that can be tested, but also, by varying propeller pitch, will allow the full motor torque vs. speed map to be explored with a single propeller to better characterize the performance of the motor and motor controller throughout the operating envelope.

Acknowledgments

This research was funded in part by the U.S. Government under National Institute of Aerospace (NIA) Cooperative Agreement Task 201201 with NASA Langley Research Center and through Task 9 of the 2021–2026 Georgia Tech Vertical Lift Research Center of Excellence (VLRCOE) grant. The U.S. Government is authorized to reproduce and distribute reprints for Government purposes notwithstanding any copyright notation thereon. The views and conclusions contained in this document are those of the authors and should not be interpreted as representing the official policies or position, either expressed or implied, of the U.S. Army Combat Capabilities Development Command (DEVCOM), Aviation & Missile Center (AvMC), NASA, or the U.S. Government. The authors would also like to acknowledge the NASA Airvolt team for their support during the design of the electrical and software systems. In addition, the authors thank Joseph Elbon, Michael Hartin, Noah Ben-Sahib, Jack Labadia and Ethan Das for their contribution to various aspects of the project.

References

[1] Kim, H. D., Perry, A. T., and Ansell, P. J., "A Review of Distributed Electric Propulsion Concepts for Air Vehicle Technology," *AIAA Paper 2018–4998*, July 2018. https://doi.org/10.2514/6.2018-4998.

[2] Samuel, A., and Lin, Y., "Airvolt Aircraft Electric Propulsion Test Stand," *AIAA Paper 2015–4108*, July 2015. https://doi.org/10.2514/6.2015-4108.

[3] Munari, B., and Schneer, A., "How to Design a Precharge Circuit for Hybrid and Electric Vehicle Applications," Tech. rep., Sensata Technologies, 2020.